Electronic Journal of Mathematics
www.shahindp.com/locate/ejm

Electron. J. Math. **11** (2026) 99–110
DOI: 10.47443/ejm.2026.007

Research Article

Dynamics of a Generalized Fractional Van der Pol System

Juan E. Nápoles Valdés[1,2,‡], Juan Cruz Vergara[1], Luana Sivori Yedro[1], Pablo F. Wagner Boián[1]

[1]*Facultad de Ciencias Exactas y Naturales y Agrimensura,*
Universidad Nacional del Nordeste, Av. Libertad 5450, Corrientes, Argentina
[2]*Facultad Regional Resistencia,*
Universidad Tecnologica Nacional, French 414, Resistencia, Chaco, Argentina

Abstract

In this work, we examine the dynamical behavior of the Van der Pol oscillator based on a local generalized derivative, which includes, as particular cases, both conformable and non-conformable derivatives depending on the kernel considered. The analysis of the model is carried out using various kernel functions and different orders, providing a high degree of generality. Numerical simulations are compared with analytical solutions to validate the approach and to highlight the impact of the different kernels and orders.

Keywords: local generalized derivative; Van der Pol oscillator; simulation.

2020 Mathematics Subject Classification: 34C15, 37N20.

1. Introduction

Over the past few decades, fractional calculus has emerged as a powerful mathematical framework for modeling complex systems with memory, hereditary properties, and nonlocal dynamics. In contrast to classical integer-order derivatives, fractional-order derivatives provide additional degrees of freedom that enable more accurate descriptions of physical, biological, and engineering processes. Applications range from viscoelastic materials and electrical circuits to biological rhythms and control theory.

A particularly fruitful direction within fractional calculus involves the use of local fractional operators, which balance the interpretability and computational tractability of classical calculus with the extended modeling capabilities of fractional-order dynamics. Among these, a local generalized derivative N_F^α (see Definition 2.1 in the next section) was proposed in [19] as a versatile tool that encompasses both conformable and non-conformable derivatives through the choice of the kernel function $F(t,\alpha)$. This approach allows for a unified treatment of a wide range of fractional models and provides flexible mechanisms to encode memory effects and time-dependent scaling.

The Van der Pol oscillator is a paradigmatic nonlinear system originally introduced to describe electrical circuits with nonlinear resistors (for instance, see [12, 14]). It is now widely used to model phenomena in neuroscience, biology, and mechanics due to its self-sustained oscillatory behavior and rich dynamical structure. Despite its simplicity, the Van der Pol system exhibits diverse dynamical regimes, including limit cycles, bifurcations, and synchronization.

Received: 14 January 2026. Received in revised form: 18 March 2026. Accepted: 2 April 2026. Published online: 6 May 2026.
‡Corresponding author (jnapoles@exa.unne.edu.ar).

In this study, we explore a fractional generalization of the Van der Pol oscillator by replacing classical derivatives with the local generalized operator N_F^α. We examine how different choices of kernel functions, including both conformable and non-conformable types, affect the qualitative and quantitative features of the oscillator's dynamics. This analysis is carried out through numerical simulations, using a Runge-Kutta method to solve the resulting fractional system for various values of the order α and the nonlinearity parameter μ.

Our aim is twofold: first, to assess the applicability and flexibility of the operator N_F^α in modeling nonlinear oscillatory systems, and second, to understand how different kernel-induced memory effects influence the long-term behavior of the Van der Pol oscillator. The obtained results highlight the sensitivity of the system to the choice of fractional kernel and derivative order, offering insights into the design of fractional models with desired dynamical characteristics.

2. Theoretical Framework

Because of their theoretical significance and practical applications, local generalized operators have attracted increasing attention from researchers since 2014. One such example is the conformable derivative of order α, which generalizes the classical derivative through a limit-based formulation (see [8]). A distinctive feature of a new local derivative introduced in 2018 (see [6, 18]) is that it does not reduce to the ordinary derivative as $\alpha \to 1$. Since the slope of the tangent line to the curve at a point is not preserved in this limit, we refer to this derivative as non-conformable, to distinguish it from previously known ones. In this case, the kernel has the form $e^{t^{-\alpha}}$ (see [6, 10, 18]).

This study builds upon theoretical developments from previous works, particularly those presented in [19], with additional context provided in [5, 23].

Definition 2.1 (Generalized Local Derivative)**.** *Let $f : [0, \infty) \to \mathbb{R}$ be a function and $\alpha \in (0, 1)$. The N-fractional derivative of order α is defined by*

$$N_F^\alpha f(t) = \lim_{\epsilon \to 0} \frac{f(t + \epsilon F(\alpha, t)) - f(t)}{\epsilon}, \tag{1}$$

where $F(\alpha, t)$ is a suitably chosen kernel function, often involving the two-parameter Mittag-Leffler function $E_{a,b}(\cdot)$.

Remark 2.2. *Definition 2.1 encompasses both conformable and non-conformable derivatives. The term "conformable" refers to derivatives that reduce to the classical derivative as $\alpha \to 1$, as in [8], whereas "non-conformable" derivatives, such as those in [6], do not satisfy this condition.*

The adoption of the generalized derivative N_F^α is motivated by its flexibility in modeling, offering two degrees of freedom: the kernel function $F(\alpha, t)$ (which determines whether the operator is conformable or not), and the order α. If a conformable kernel is chosen and $\alpha = 1$, the operator reduces to the standard first-order derivative. To explore this flexibility, the present work considers a total of four kernel functions: one conformable (distinct from that of [8], which has been extensively studied), and three non-conformable kernels. This framework highlights the strength and versatility of the proposed generalized derivative.

Theorem 2.3. *Let f be differentiable in the generalized sense at $t > 0$, with $\alpha \in (0, 1]$. Then the following identity holds:*

$$N_F^\alpha f(t) = F(t, \alpha) f'(t). \tag{2}$$

As shown in [19], solutions to differential equations involving global fractional derivatives D^{α} may exhibit self-intersecting trajectories, a behavior not typically seen in integer-order systems. In contrast, when employing the local generalized operator N_F^{α}, such intersections are avoided under classical conditions of existence and uniqueness, except at critical points.

Previous studies (for example, see [2–7, 10, 17, 19, 20, 22]) have investigated several local differential operators, demonstrating their applicability across various physical and engineering systems. This growing body of work underscores the potential of generalized calculus as a powerful framework for modeling complex dynamical behavior.

2.1. Van der Pol Oscillator

The Van der Pol oscillator[§] is a non-conservative stable oscillator with nonlinear damping; in simple terms, the Van der Pol oscillator is a *self-excited oscillator with nonlinear damping*.

Before Van der Pol, most known oscillators (such as the pendulum or the simple LC circuit) were described by linear equations or by linear (friction-type) damping. In such systems:

- if the damping is positive, the oscillations decay and the system approaches an equilibrium point;
- if the damping is negative, the oscillations grow without bound.

The Van der Pol oscillator introduced a fundamentally different behavior, known as the **limit cycle**. A limit cycle is an isolated periodic trajectory in the phase plane. Solutions that begin near this cycle are attracted to it, while solutions that begin far from it (or even from deep within it) are also attracted to it. This means that the system achieves a periodic and stable oscillation with a fixed amplitude and frequency, regardless of the initial conditions. In essence, the oscillation is self-excited and self-limiting due to the underlying nonlinearity.

On the other hand, the Van der Pol equation (and its variations) has proven to be exceptionally useful for modeling real systems in which oscillations remain stable as a result of nonlinear effects, such as in electrical engineering, biology and medicine, and physics.

The Van der Pol equation became a canonical example for the study of nonlinear dynamical systems. It was one of the motivations for the development of fundamental mathematical tools, such as the Poincaré–Bendixson Theorem, which is used to establish the existence of limit cycles in the phase plane. Moreover, it serves as a bridge between the well-understood theory of linear oscillations and the more complex theory of nonlinear oscillations, which is essential for understanding chaos and complex dynamical behavior.

The Van der Pol equation is a second-order ordinary differential equation:

$$\ddot{x} - \mu\left(1 - x^2\right)\dot{x} + x = 0 \tag{3}$$

where μ is the damping constant. If $\mu = 0$, then we recover simple harmonic oscillations, whereas for $\mu > 0$, the system exhibits non-harmonic limit cycle oscillations. Equation (3) can be reduced to a system of equations by setting $y = \dot{x}$ as follows:

$$\begin{aligned} \dot{x} &= y, \\ \dot{y} &= \mu\left(1 - x^2\right) y - x. \end{aligned}$$

[§]Historical details about the Van der Pol Equation can be found in [12, 14]. Results guaranteeing various qualitative properties of its solutions can be found in [9, 11, 13, 15, 16].

2.2. Fractional Van der Pol Model

To generalize the Van der Pol dynamics, we introduce the operator

$$N_F^\alpha x(t) = F(t,\alpha)\,\frac{dx(t)}{dt},$$

where $F(t,\alpha)$ is a chosen kernel function. The following four choices of $F(t,\alpha)$ are considered:

1. $F(t,\alpha) = t^\alpha$ (non-conformable kernel),
2. $F(t,\alpha) = t^{-\alpha}$ (non-conformable kernel),
3. $F(t,\alpha) = e^{t-\alpha}$ (non-conformable kernel),
4. $F(t,\alpha) = e^{t(1-\alpha)}$ (conformable kernel).

These kernels replace the usual derivative to form a fractional-like differential operator. In this framework, one can write a fractional Van der Pol equation by replacing ordinary derivatives with N_F^α. For instance, applying N_F^α to the velocity yields a second-order form:

$$N_F^\alpha(\dot{x}(t)) - \mu(1-x(t)^2)\dot{x}(t) + x(t) = 0. \tag{4}$$

Since

$$N_F^\alpha(\dot{x}(t)) = F(t,\alpha)\,\ddot{x}(t),$$

we have

$$F(t,\alpha)\,\ddot{x}(t) - \mu(1-x(t)^2)\dot{x}(t) + x(t) = 0. \tag{5}$$

Dividing by $F(t,\alpha)$, we obtain the following fractional Van der Pol differential equation in standard form:

$$\ddot{x}(t) = \frac{\mu(1-x(t)^2)\dot{x}(t) - x(t)}{F(t,\alpha)}. \tag{6}$$

In an equivalent first-order formulation, obtained by setting $y = \dot{x}$, one may write

$$\begin{cases} N_F^\alpha x(t) = F(t,\alpha)\dot{x}(t) = y(t), \\ N_F^\alpha y(t) = F(t,\alpha)\dot{y}(t) = \mu(1-x(t)^2)y(t) - x(t). \end{cases} \tag{7}$$

Hence, the system becomes

$$\begin{cases} \dot{x}(t) = \dfrac{y(t)}{F(t,\alpha)}, \\ \dot{y}(t) = \dfrac{\mu(1-x(t)^2)y(t) - x(t)}{F(t,\alpha)}, \end{cases} \tag{8}$$

with initial conditions $x(0) = x_0$ and $y(0) = y_0$. This "fractionalized" Van der Pol model reduces to the standard oscillator when $F(t,\alpha) = 1$. Studying its behavior allows one to explore how different kernel choices affect the amplitude, frequency, and stability of the limit cycle.

3. Results

In Figure 3.1, we illustrate the asymptotic behavior of the Van der Pol oscillator through phase portraits for different values of the nonlinearity parameter μ. In this case, the kernel $F(t,\alpha) = \exp[t(1-\alpha)]$ is considered with $\alpha = 0.25$ and $\alpha = 0.75$, and the results are compared with those obtained using the ordinary derivative. In both regimes, the system rapidly approaches a stable state, which is consistent with the behavior of the kernel for large values of time.

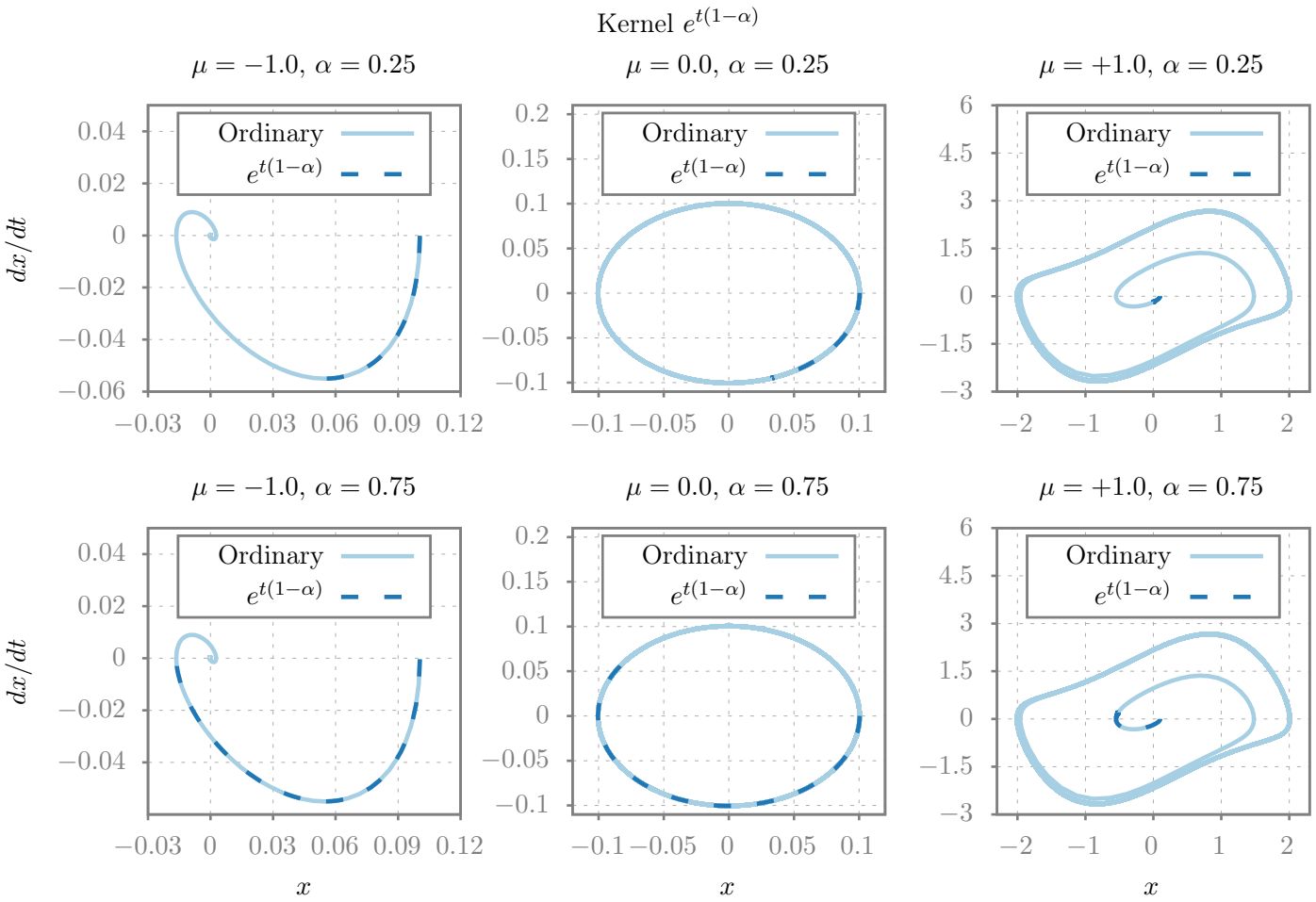

Figure 3.1: Phase diagram of the Van der Pol oscillator using the kernel $F(t,\alpha) = \exp[t(1-\alpha)]$ for $\mu = -1, 0, +1$ and $\alpha = 0.25, 0.75$.

Next, in Figure 3.2, we compare the ordinary derivative with the nonconformable case corresponding to the kernel $F(t,\alpha) = t^{\alpha}$ in the same regimes. Although the qualitative behavior of the solutions does not change, for larger values of α the dynamics of the system evolve more slowly.

Moving now to the kernel $F(t,\alpha) = t^{-\alpha}$ (see Figure 3.3), the system appears to gain energy when $\mu = 0$, that is, when it reduces to a harmonic oscillator without a damping term. This effect is suppressed for $\mu = -1$ due to the spiral nature of the fixed point and also for $\mu = 1$ because the additional energy drives the system further into the limit cycle.

In Figure 3.4, we present the same phase portrait using the kernel $F(t,\alpha) = \exp[t^{-\alpha}]$, compared with the ordinary derivative. The solutions exhibit similar behavior in both regimes.

We now turn to the position–time plots. For a negative nonlinearity parameter $\mu = -1$ (see Figure 3.5), all solutions converge to a fixed point at different rates. The kernel $F(t,\alpha) = t^{-\alpha}$ leads to the fastest convergence, while $F(t,\alpha) = t^{\alpha}$ results in the slowest. The kernel $F(t,\alpha) = \exp[t(1-\alpha)]$ is particularly interesting, as the solutions $x(t)$ approach a steady state that depends on the order α of the derivative.

For $\mu = 0$ (see Figure 3.6), and for the kernel $F(t,\alpha) = \exp[t(1-\alpha)]$, we again observe an order-dependent steady state of $x(t)$. Using the kernel $F(t,\alpha) = t^{-\alpha}$, the solution clearly diverges for large values of time, which is consistent with the increasing orbit sizes observed in the phase portrait. For both kernels $F(t,\alpha) = t^{\alpha}$ and $F(t,\alpha) = \exp[t^{-\alpha}]$, the solutions exhibit similar behavior, differing mainly in the number of oscillations, which is also dependent on the order α.

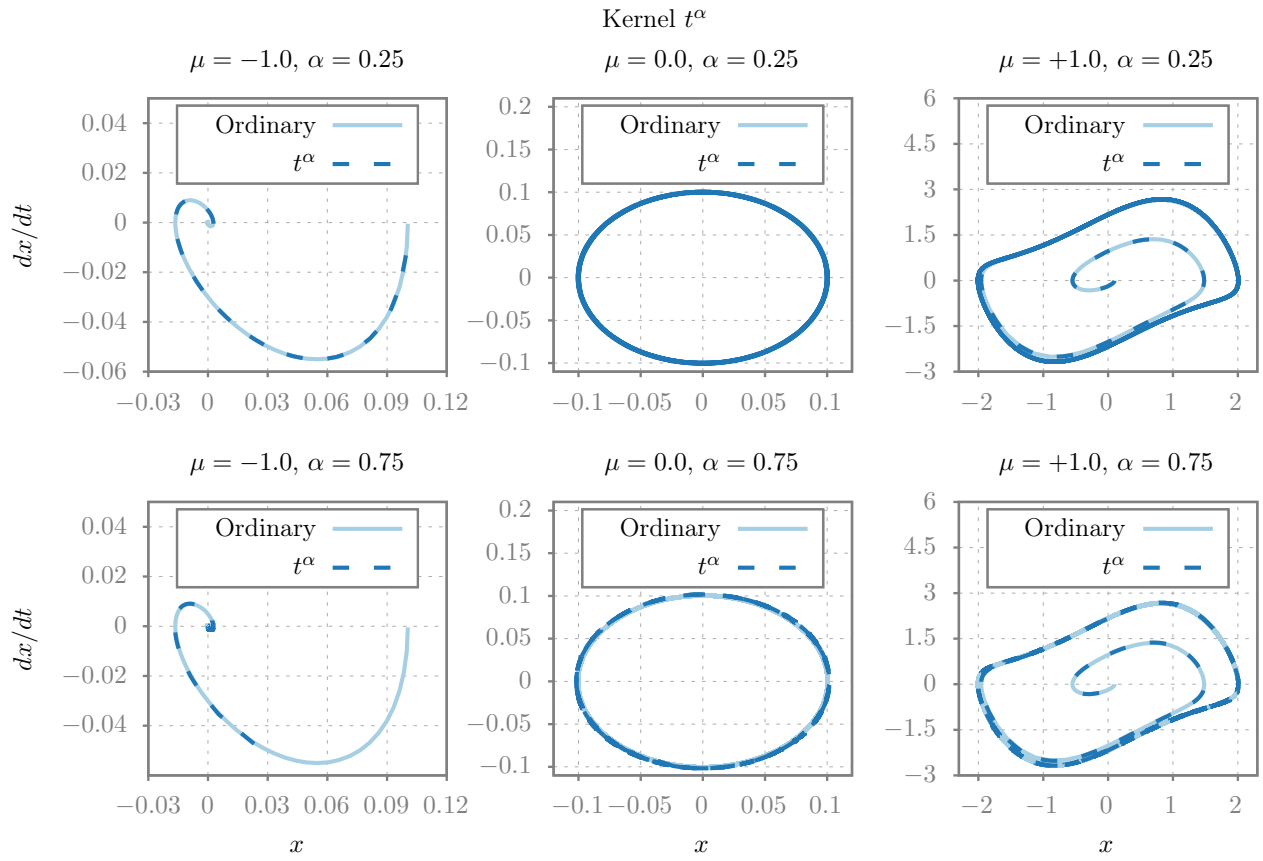

Figure 3.2: Phase diagram of the Van der Pol oscillator using the kernel $F(t, \alpha) = t^\alpha$ for $\mu = -1, 0, +1$ and $\alpha = 0.25, 0.75$.

Finally, Figure 3.7 presents a similar behavior for $\mu = 1$ with the kernel $F(t, \alpha) = \exp[t(1 - \alpha)]$, showing steady states that depend on the order α. The remaining kernels do not significantly alter the qualitative behavior of the solutions, except for changes in the oscillation frequency. In particular, for the kernel $F(t, \alpha) = t^{-\alpha}$, the system rapidly reaches the limit cycle and $x(t)$ exhibits oscillations with a regular amplitude.

In general, we observe that the dynamics of the fractional Van der Pol oscillator are strongly influenced by the nonlinearity parameter μ, the order of the derivative α, and the choice of kernel $F(t, \alpha)$.

- **Effect of μ:**
  - ▷ For $\mu = -1$, the system converges to a fixed point, with the rate of convergence depending on the kernel.
  - ▷ For $\mu = 0$, corresponding to the linear (harmonic) oscillator, some kernels (notably the kernel $F(t, \alpha) = t^{-\alpha}$) lead to energy growth over time.
  - ▷ For $\mu = 1$, the system develops a stable limit cycle. The kernel influences the rate at which this limit cycle is reached but does not affect its existence.
- **Effect of α:**
  - ▷ Lower values of α introduce stronger memory effects, generally slowing down the system's evolution or increasing damping.
  - ▷ As α approaches 1, the behavior becomes closer to that of the classical derivative.

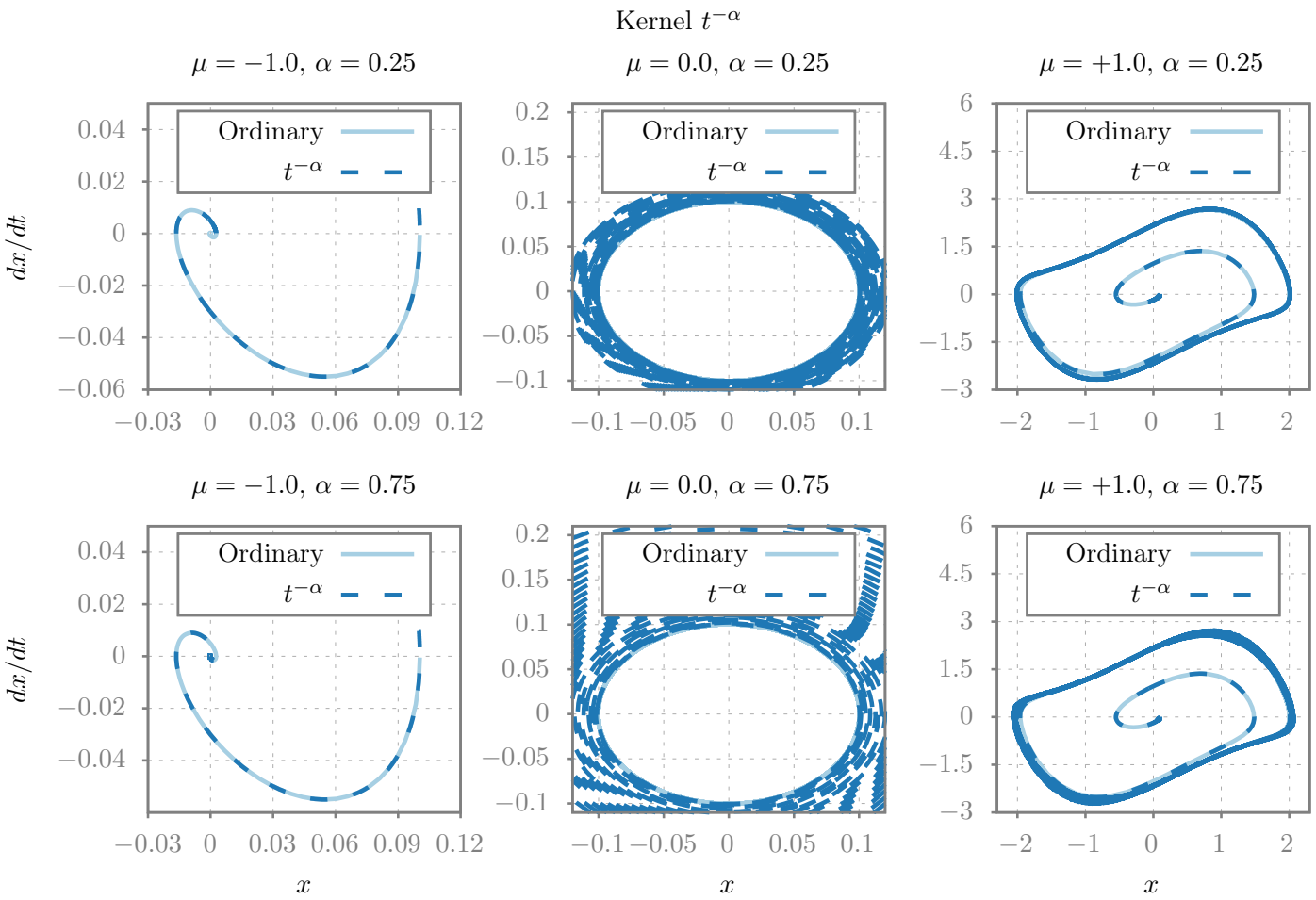

Figure 3.3: Phase diagram of the Van der Pol oscillator using the kernel $F(t,\alpha) = t^{-\alpha}$ for $\mu = -1, 0, +1$ and $\alpha = 0.25, 0.75$.

- **Effect of the kernel $F(t,\alpha)$:**
  - ▷ $F(t,\alpha) = t^{\alpha}$: slows down the dynamics; the system evolves more slowly for larger α.
  - ▷ $F(t,\alpha) = t^{-\alpha}$: accelerates the dynamics and, in some cases (e.g., $\mu = 0$), leads to unbounded growth.
  - ▷ $F(t,\alpha) = \exp[t(1-\alpha)]$: produces α-dependent steady states; its influence is particularly noticeable in the transient regime.
  - ▷ $F(t,\alpha) = \exp[t^{-\alpha}]$: exhibits behavior close to the classical case, with only slight variations in oscillation frequency and amplitude.

4. Computational Procedure

The computational procedure used to study the dynamics of the fractional Van der Pol oscillator with different kernel functions is described below. This approach combines numerical simulations with semi-analytical solutions to analyze how the fractional parameters and the choice of a kernel influence the system's behavior.

The analysis begins by defining the kernel functions that describe the fractional properties of the system. Four functions are considered to explore their effects on the dynamics: t^{α}, $t^{-\alpha}$, $e^{t^{-\alpha}}$, and $e^{t(1-\alpha)}$. These functions are selected because they represent different types of relationships with t and α, allowing for a detailed comparison between algebraic and exponential kernels, as well as between long- and short-memory behaviors.

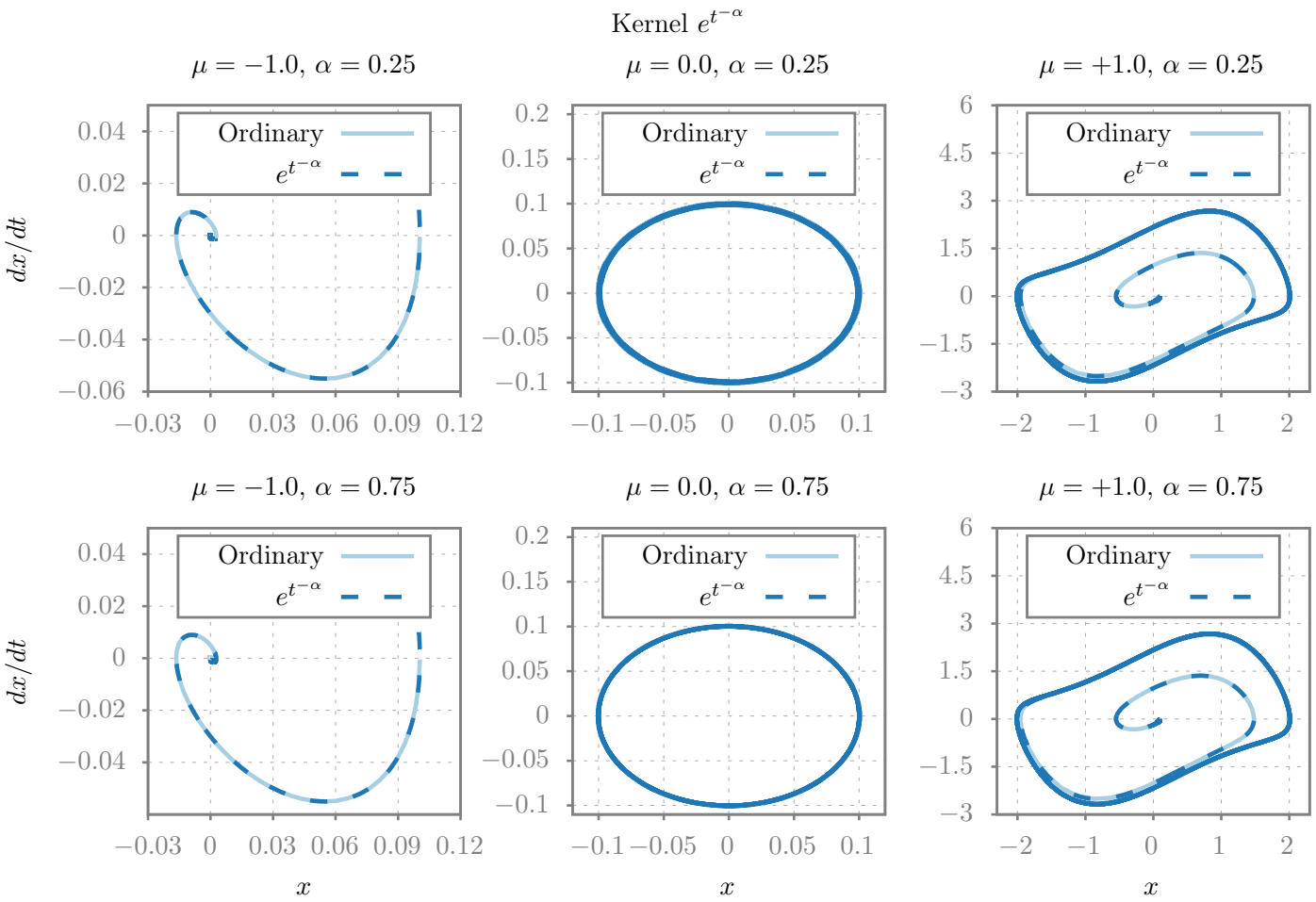

Figure 3.4: Phase diagram of the Van der Pol oscillator using the kernel $F(t,\alpha) = \exp[t^{-\alpha}]$ for $\mu = -1, 0, +1$ and $\alpha = 0.25, 0.75$.

To solve the fractional Van der Pol equation, the classical fourth-order Runge–Kutta (RK4) method is used. This method is implemented in `Fortran` and is designed to integrate systems of ordinary differential equations with high accuracy. The RK4 algorithm computes four intermediate values (k_1, k_2, k_3, k_4) at each time step to update the state of the system. These values are calculated as follows:

$$k_1 = hf(y), \quad k_2 = hf\left(y + 0.5\,k_1\right), \quad k_3 = hf\left(y + 0.5\,k_2\right), \quad k_4 = hf\left(y + k_3\right),$$

where h is the time step, f represents the governing function of the system, and y denotes the state variables. A step size of $h = 0.001$ is chosen to ensure accurate results over the entire simulation time.

The fractional Van der Pol oscillator is described by the system:

$$\frac{dx}{dt} = y, \qquad \frac{dy}{dt} = \frac{\mu(t)}{F(t,\alpha)}(1 - x^2)y - x,$$

where $\mu(t)$ is the time-dependent damping parameter, taken as $\mu(t) = t$, and $F(t,\alpha)$ is the kernel function that introduces memory effects into the dynamics. This formulation extends the classical Van der Pol model by incorporating fractional-order behavior through the kernel.

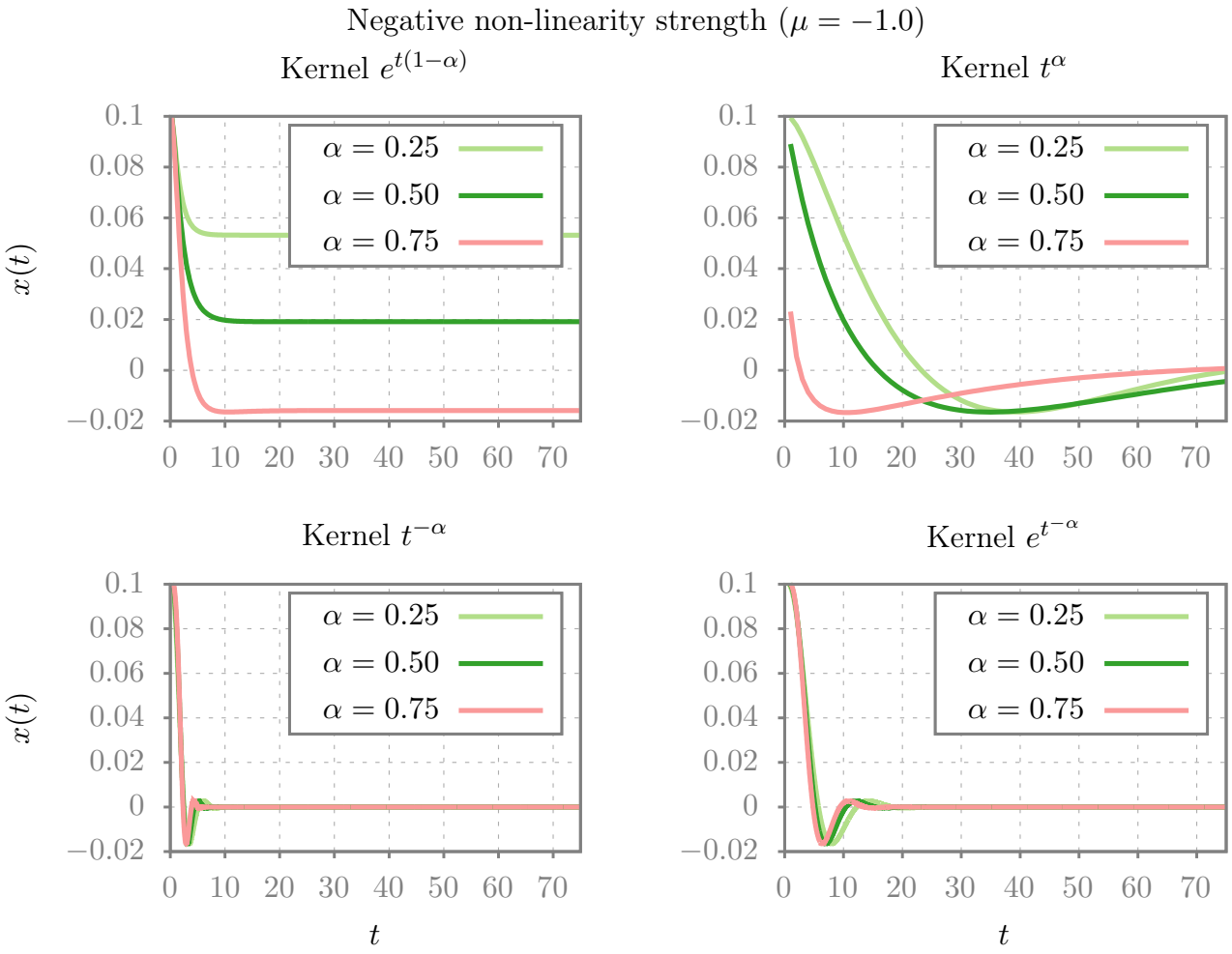

Figure 3.5: Position versus time for the Van der Pol oscillator with different derivative orders and kernels for the negative nonlinearity parameter $\mu = -1$.

To account for differences in the rates at which each kernel drives the system's evolution, appropriate adjustments were made to the simulation time intervals. Some kernels, especially those exhibiting sharper or faster-varying behavior, require smaller time steps and longer integration times to accurately capture their effects on the dynamics. In contrast, kernels associated with slower or smoother evolution allow for coarser time resolution without significant loss of detail. Accordingly, both the time step and the total simulation duration were scaled depending on the kernel used. This approach ensures that each simulation achieves a balance between precision and computational efficiency, enabling meaningful comparisons between kernels with markedly different dynamical characteristics.

Simulations were performed for three different values of the fractional order ($\alpha = 0.25$, $\alpha = 0.50$, and $\alpha = 0.75$) across all kernel functions. The initial conditions were set as $x_0 = 0.1$, $y_0 = 0.01$, and $t_0 = 0.001$. The RK4 integrator, using a step size of $h = 0.001$, was applied to calculate the evolution of the system over time. The results, including both time series and phase-space trajectories, were saved for further analysis.

The numerical and reference solutions were compared through plots for each kernel function, showing how $x(t)$ and $y(t)$ evolve for different values of α. Solid lines represent the RK4 results, while dashed lines correspond to the high-precision solutions. These plots highlight the accuracy of the numerical method and illustrate the impact of each kernel function on the system's transient and long-term dynamics.

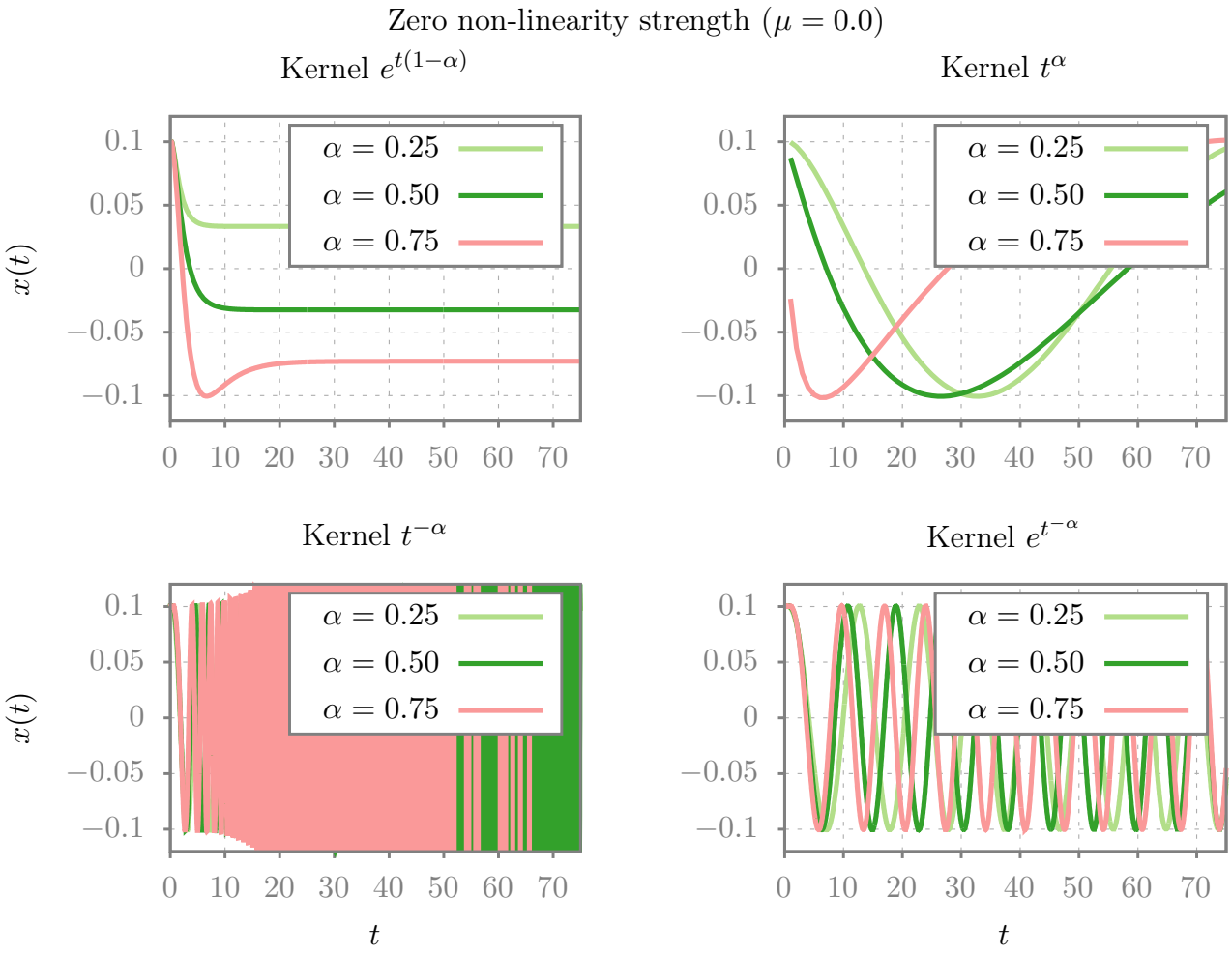

Figure 3.6: Position versus time for the Van der Pol oscillator with different derivative orders and kernels for the case $\mu = 0$, corresponding to a harmonic oscillator.

5. Conclusions

This work has shown the dynamics of the generalized Van der Pol oscillator by replacing the classical derivative with the fractional local operator N_F^{α}. The introduction of the generalized local derivative N_F^{α} allowed for a unified treatment of conformable and non-conformable fractional models through the selection of the kernel $F(t, \alpha)$. This approach offers two crucial degrees of freedom (the order α and the kernel function) for tuning the system dynamics.

Numerical simulations confirmed that the dynamics of the fractional Van der Pol oscillator are strongly influenced by three factors: the nonlinearity parameter μ, the order of the derivative α, and the choice of the kernel $F(t, \alpha)$.

For $\mu = -1$, the system consistently converges to a fixed point, but the convergence rate varies significantly depending on the kernel.

For $\mu = 1$, the stable limit cycle characteristic of the Van der Pol oscillator is preserved, although the kernel and the order α influence the rate at which it is reached.

For $\mu = 0$ (harmonic oscillator), the kernel $F(t, \alpha) = t^{-\alpha}$ leads to unbounded growth of the solution (explosive behavior), indicating a gain of energy over time.

The conformable kernel $F(t, \alpha) = e^{t(1-\alpha)}$ showed a remarkable result: the solutions $x(t)$ reach a steady state that depends on the order α of the derivative for $\mu = -1$, $\mu = 0$, and $\mu = +19$.

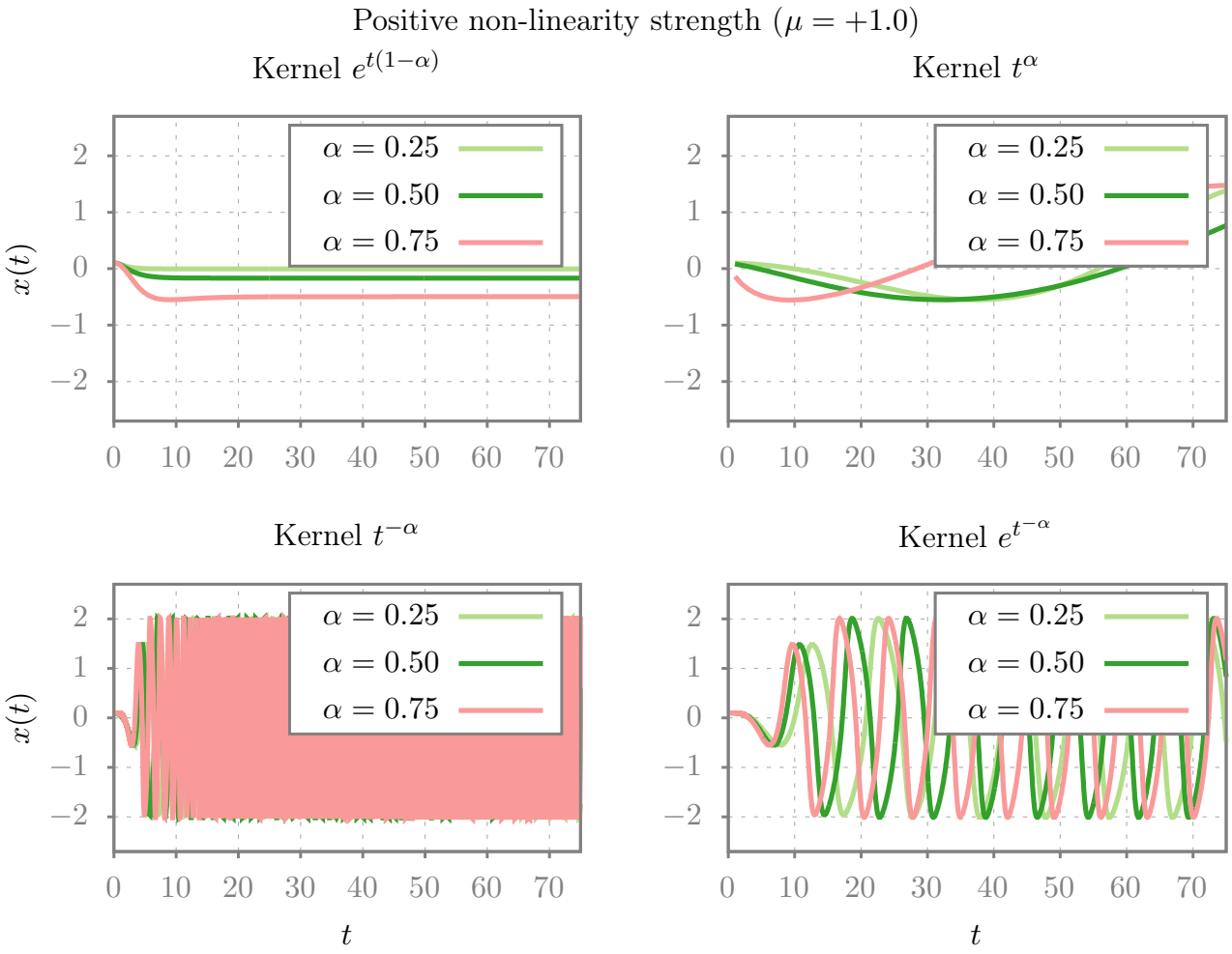

Figure 3.7: Position versus time for the Van der Pol oscillator with different derivative orders and kernels for the positive nonlinearity parameter $\mu = 1$.

The non-conformable kernel $F(t, \alpha) = t^{\alpha}$ slows down the system's dynamics, with the evolution becoming slower for larger values of α. On the other hand, the non-conformable kernel $F(t, \alpha) = t^{-\alpha}$ accelerates the dynamics and causes unbounded growth for $\mu = 0$.

The non-conformable exponential kernel $F(t, \alpha) = e^{t^{-\alpha}}$ produces minimal deviations from the classical case of the ordinary derivative, only slightly affecting the oscillation frequency and amplitude.

In summary, the choice of the kernel $F(t, \alpha)$ is fundamental, as it not only introduces memory effects but also qualitatively and quantitatively modifies the transient and asymptotic characteristics of the system, providing a powerful tool for designing fractional models with desired dynamics. This opens new directions for research involving other local operators introduced in recent years, such as those defined in [1, 7, 22].

References

[1] R. E. Castillo, J. E. Nápoles Valdés, H. Chaparro, Omega derivative, *Gulf J. Math.* **16** (2024) 55–67.

[2] G. E. Chatzarakis, J. E. Nápoles Valdés, Continuability of Liénard's type system with generalized local derivative, *Discontinuity Nonlinearity Complex.* **12** (2023) 1–11.

[3] K. Chen, W. Zhang, Study on a new fractional logistic model via deformable fractional derivative, *IAENG Int. J. Appl. Math.* **54** (2024) 1540–1544.

[4] A. Fleitas, J. A. Méndez-Bermúdez, J. E. Nápoles Valdés, J. M. Sigarreta Almira, On fractional Liénard-type systems, *Rev. Mex. Fís.* **65** (2019) 618–625.

[5] A. Fleitas, J. E. Nápoles Valdés, J. M. Rodríguez, J. M. Sigarreta, Note on the generalized conformable derivative, *Rev. Un. Mat. Argentina* **62** (2021) 443–457.

[6] P. M. Guzmán, G. E. Langton, L. M. Lugo Motta Bittencourt, J. Medina, J. E. Nápoles Valdés, A new definition of a fractional derivative of local type, *J. Math. Anal.* **9** (2018) 88–98.

[7] P. M. Guzmán, J. E. Nápoles Valdés, M. Vivas-Cortez, A new generalized derivative and related properties, *Appl. Math. Inf. Sci.* **18** (2024) 923–932.

[8] R. Khalil, M. Al Horani, A. Yousef, M. Sababheh, A new definition of fractional derivative, *J. Comput. Appl. Math.* **264** (2014) 65–70.

[9] L. Lugo, S. Noya, J. E. Nápoles Valdés, On the construction of regions of stability, *Pure Appl. Math. J.* **3** (2014) 87–91.

[10] F. Martínez, J. E. Nápoles Valdés, Towards a non-conformable fractional calculus of n-variables, *J. Math. Appl.* **43** (2020) 87–98.

[11] J. E. Nápoles Valdés, A continuation result for a bidimensional system of differential equations, *Rev. Integración* **13** (1995) 49–54.

[12] J. E. Nápoles Valdés, The historical legacy of ordinary differential equations, *Boletín Mat.* **5** (1998) 53–79.

[13] J. E. Nápoles Valdés, A note on the asymptotic stability in the whole of non-autonomous systems, *Rev. Colomb. Mat.* **33** (1999) 1–8.

[14] J. E. Nápoles Valdés, A century of qualitative theory of differential equations, *Lect. Mat.* **25** (2004) 59–111.

[15] J. E. Nápoles Valdés, On the existence of periodic solutions of some generalized Liénard type systems, *Math. Sci. Res. J.* **15** (2011) 115–126.

[16] J. E. Nápoles Valdés, A note on the qualitative behavior of some second order nonlinear equation, *Appl. Appl. Math.* **8** (2013) 767–776.

[17] J. E. Nápoles Valdés, A. R. Brisa, S. Lautaro, M. A. F. Moragues, Numerical simulation of local generalized derivative for a harmonic oscillator, *J. Phys. Appl. Mech.* **1** (2022) #1003.

[18] J. E. Nápoles Valdés, P. M. Guzmán, L. M. Lugo, Some new results on nonconformable fractional calculus, *Adv. Dyn. Syst. Appl.* **13** (2018) 167–175.

[19] J. E. Nápoles Valdés, P. M. Guzmán, L. M. Lugo, A. Kashuri, The local generalized derivative and Mittag–Leffler function, *Sigma J. Eng. Nat. Sci.* **38** (2020) 1007–1017.

[20] J. E. Nápoles Valdés, P. M. Roa, Numerical simulations in a generalized Liénard's type system, *Ann. Math. Phys.* **6** (2023) 187–195.

[21] I. Owusu-Mensah, L. Akinyemi, B. Oduro, O. S. Iyiola, A fractional order approach to modeling and simulations of the novel COVID-19, *Adv. Differ. Equ.* (2020) #683.

[22] M. Vivas-Cortez, L. M. Lugo, J. E. Nápoles Valdés, M. E. Samei, A multi-index generalized derivative: some introductory notes, *Appl. Math. Inf. Sci.* **16** (2022) 883–890.

[23] D. Zhao, M. Luo, General conformable fractional derivative and its physical interpretation, *Calcolo* **54** (2017) 903–917.